On the Stability Crossing Boundaries of Some Delay Systems Modeling Immune Dynamics in Leukemia

Silviu-Iulian Niculescu, Peter S. Kim, Keqin Gu, Doron Levy

***Abstract*— This paper focuses on the characterization of delay effects on the asymptotic stability of some continuous-time delay systems encountered in modeling the post-transplantation dynamics of the immune response to chronic myelogenous leukemia. More explicitly, we shall discuss the stability of the crossing boundaries of the corresponding linearized models in the delay-parameter space. Weak, and strong cell interactions are discussed, and analytic characterizations are proposed. An illustrative example completes the presentation.**

***Keywords*— Delay; asymptotic stability; switch; reversal; crossing curves; quasipolynomial.**

I. Introduction

The stability analysis of population dynamics and of physiology models (specially, dynamic diseases) in presence of time-delays is a subject of recurring interest (see, for instance, [14], [15], [17], and the references therein), since the delays are *inherent* in the model representation (maturity, gestation are never instantaneous process), and since their presence may induce *complex behaviors* (instability, oscillations, chaotic behaviors).

A. Nonlinear delay model

In the sequel, we shall consider the following nonlinear model proposed by [7], [13] to describe the post-transplantation dynamics of the immune response to chronic myelogenous leukemia:

$$\begin{cases} \dfrac{dT(t)}{dt} = -d_T T(t) - kC(t)T(t) \\ \qquad +p_2 kC(t-\sigma)T(t-\sigma) \\ \qquad +2^N p_1 q_1 kC(t-\rho-N\tau)T(t-\rho-N\tau) \\ \qquad +p_1 q_2 kC(t-\rho-\upsilon)T(t-\rho-\upsilon) \\ \dfrac{dC(t)}{dt} = rC(t)\left(1-\dfrac{C(t)}{K}\right) \\ \qquad -\tilde{p}_1 kC(t-\rho)T(t-\rho), \end{cases} \tag{1}$$

Silviu-Iulian Niculescu is with HEUDIASYC (UMR CNRS 6599), Université de Technologie de Compiègne, Centre de Recherche de Royallieu, BP 20529, 60205, Compiègne, France; Corresponding author at phone: +33.3.44.23.44.84, fax: +33.3.44.23.44.77, E-mail: niculescu@hds.utc.fr. The research of S.-I. Niculescu is partially funded by a CNRS-USA Grant: "Delays in interconnected systems: Analysis, and applications" (2005–2008).

Peter S. Kim is with the Department of Mathematics, Stanford University, California, USA. E-mail: pkim@math.stanford.edu

Keqin Gu is with the Department of Mechanical and Industrial Engineering, Southern Illinois University at Edwardsville, Edwardsville, Illinois, 62026-1805, USA. E-mail: kgu@siue.edu

Doron Levy is with the Department of Mathematics, Stanford University, California, USA. E-mail: dlevy@math.stanford.edu. The research of D. Levy is partially supported by the NSF under Career Grant DMS-0133511

where the variable T refers to the anti-cancer cell population, and C refers to the cancer cell population, both functions of time t. All the other variables are constant and non-negative. The constants p_i, q_i, and $\tilde{p}_i$ are probabilities between 0 and 1. Furthermore, $p_1 + p_2 = 1$, and $0 \leq q_1 + q_2 \leq 1$.

The various stages of the evolution of cancer cells and of T cells are demonstrated in Figures 1 and 2. Cancer cells have a logistic growth rate and a decrease in their population as a result of the interaction with T cells. T cells can interact with cancer cells, in which case they either decide to ignore them and return to the general T cell population after a delay σ or react with cancer cells and eliminate them. In this case they either die, or return to the general cell population. A return to the general population can occur with or without a proliferation. In addition, there is a natural death rate of T cells that is included in the model. The natural death rate of cancer cells is already taken into account in the logistic growth term.

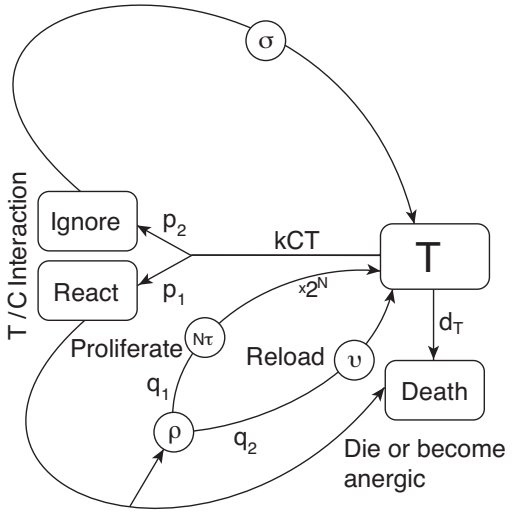

Fig. 1. Evolution of anti-cancer T cells

The original model tracks the time evolution of six cell populations (cancer cells, anti-donor T cells, general patient blood cells, anti-host T cells, anti-cancer T cells, and general donor blood cells). The interaction between the anti-cancer T cells from the donor and the cancer cells in the host is the most important, since these T cells primarily eliminate cancer cells in the host. Hence, to simplify stability analysis, we consider the reduced system (1). In

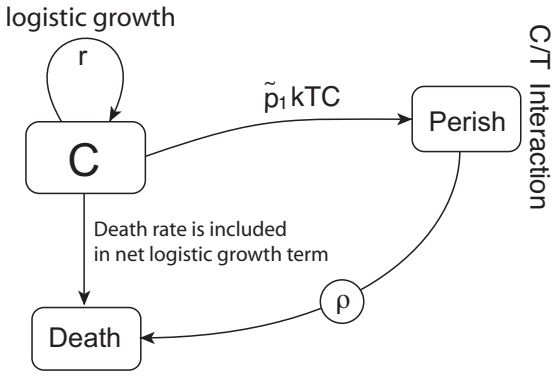

Fig. 2. Evolution of cancer C cells

addition, a time-delay model offers a unique advantage in immune system modeling, because delays provide means for dealing with programmed T cell responses. When stimulated by a target, T cells undergo a program of division even if the original stimulation is removed [4]. Thus, the overall immune response at a given time is not dependent upon the current level of the stimulus, but on the level at some time in the past [18].

B. Delay description

In the system (1) above, there are *four distinct delays*, namely σ, $\rho + N\tau$, $\rho + \upsilon$, and ρ. The relevant values are approximately

1) $\sigma = 0.0007$ days $= 1$ min
2) $\rho = 0.0035$ days $= 5$ min
3) $\tau = 1$ day
4) $\upsilon = 1$ day
5) N is between 1 and 8 and probably close to 3.

These constants respectively represent the time for unreactive interactions between T cells and cancer cells (σ), the time for reactive interactions (ρ), the time for one round of cell division (τ), the T cell recovery time after killing a cancer cell (υ), and the average number of T cell divisions after stimulation (N).

C. Crossing boundaries

Stability analysis is appropriate for this model, because a stable solution implies full remission of cancer or a controlled state, corresponding to a successful bone marrow transplant. On the other hand, an unstable solution implies the eventual relapse of the cancer population, corresponding to an unsuccessful transplant.

In the sequel, we are interested in analyzing the *effects* induced by the *delays presence* on the (asymptotic) stability of the corresponding linearized model, and more explicitly to derive the *stability/instability mechanisms* in the delay-parameter space. More precisely, we are interested in analyzing the effect induced by the *large delays* υ, and $N\tau$ on the stability boundaries[1], and in characterizing the *interactions* between *large* and *small* delays. In other words, we are interested in analyzing the *stability crossing boundaries* in the delay-parameter space defined by the large delays $N\tau$, and υ.

It is well known from the literature that such a stability characterization problem is still *open* in the general linear case (see, for instance, [8]), and that it is $\mathcal{NP}$-hard from the computational point of view [21]. However, the *particular structure* of the system, together with the particular way in which the *delays* appear in the differential equations, allow the *characterization* of the stability crossing boundaries in the delay-parameter space.

As presented above (nonlinear model), the large delays $N\tau$, and υ describe the *T/C interactions*. Without any loss of generality, we can define two types of interactions: *weak*, and *strong* T/C interactions. The *weak interaction* simply corresponds to the situation when the large delays $N\tau$, and υ have a very low impact on the stability behavior, and the stability property will be very sensitive to the parameter variations of the small delay values. By complementarity, the *strong interaction* will describe the situation in which the stability of the model is *sensitive* also to the large delays $N\tau$, and υ. Connections with delay-independent/delay-dependent (stability) type properties will be also presented. Based on these simple remarks, it seems that *strong T/C interactions* will be more difficult to characterize, and present more interest. Finally, it is important to point out that an increased (average) number of T cell division after stimulation will significatively affect the behavior of the crossing boundaries, and the T/C interactions become more significant. In order to complete the presentation, a *measure* for *weak T/C interactions* will be derived. Such a measure will be *computationally tractable*, and will allow *defining* properly the cases when a T/C interaction has a *weak* or *strong character*.

As seen below, we can rewrite the linearized model in some nice, and appealing way, that allows using a simple *geometrical idea* (as suggested by some of the authors of this note in [10] for some class of quasipolynomials including two *independent* delays) for defining the frequency crossing set (all frequencies corresponding to all the points in the stability crossing curves). However, the approach in [10] cannot be applied directly to the case study under consideration, and the definition of the *crossing set* here is more complicated.

Next, this crossing set will allow the characterization of the *stability crossing curves* in the delay-parameter space defined by the large delays υ, and $N\tau$, that is a series of smooth curves excepting some degenerate cases to be considered. The classification of the boundaries will be done in the light of the approach considered by [10] (see Section III). The novelty with respect to [10] is the use of more general analytic functions, and the particular way to treat the *small delays* σ, and ρ. Furthermore, the approach considered here will allow the analytic characterization of weak/strong T/C interactions. As mentioned above, we will

[1]For example, it is important to note that the second large delay has a relatively large range, $\tau \leq N\tau \leq 8\tau$.

give the explicit computation of some quantitative measure that characterizes weak T/C interaction.

The presentation will be as simple as possible, focusing more on the main mathematical ideas (and less on complete proofs), and the related interpretations of the results in terms of post-transplantation dynamics of the immune response to chronic myelogenous leukemia.

The remaining paper is organized as follows: Section II is devoted to some preliminary results, and to various interpretations needed in the next paragraphs. The main results are presented in Section III, and some illustrative example is discussed in Section IV. Finally, some concluding remarks end the paper. The notations are standard.

II. Preliminary results, and interpretations

We start by deriving the linearized model of the system (1), and next we discuss its stability in the case free of delays. The particular structure of the linearized model leads to a nice form of the corresponding characteristic equation in the presence of delays. Its structure will allow defining some appropriate *auxiliary system* including *small delays* needed in the next section to complete the analysis.

For convenience, let

$$\begin{array}{lll} b_1 = d_T, & b_5 = p_1 q_2 k, & \tilde{\tau} = \rho + N\tau, \\ b_2 = k, & c_1 = r, & \tilde{\upsilon} = \rho + \upsilon, \\ b_3 = p_2 k, & c_2 = r/K, & \\ b_4 = 2^N p_1 q_1 k, & c_3 = \tilde{p}_1 k, & \end{array} \tag{2}$$

and rewrite (1) as

$$\begin{cases} \frac{dT(t)}{dt} = -b_1 T(t) - b_2 C(t) T(t) \\ \qquad\quad +b_3 C(t-\sigma) T(t-\sigma) \\ \qquad\quad +b_4 C(t-\tilde{\tau}) T(t-\tilde{\tau}) \\ \qquad\quad +b_5 C(t-\tilde{\upsilon}) T(t-\tilde{\upsilon}), \\ \frac{dC(t)}{dt} = c_1 C(t) - c_2 C(t)^2 - c_3 C(t-\rho) T(t-\rho). \end{cases} \tag{3}$$

For future reference, we note that all parameters in (2) are positive. Let $b = -b_2 + b_3 + b_4 + b_5$. Then the fixed points, (T_0, C_0), of (3) are solutions to

$$\begin{cases} 0 &= -b_1 T_0 + b C_0 T_0 = (-b_1 + b C_0) T_0, \\ 0 &= (c_1 - c_2 C_0 - c_3 T_0) C_0, \end{cases}$$

i.e., the three fixed points are $(T_0, C_0) = (0,0)$, $\left(0, \frac{c_1}{c_2}\right)$, and $\left(\frac{c_1 - c_2 b_1/b}{c_3}, \frac{b_1}{b}\right)$.

The fixed point $(0,0)$ represents the ideal outcome, where the cancer population is entirely eliminated and the cancer-reactive T cells become unnecessary and disappear. Unfortunately, we will later show that this fixed point is a *saddle* regardless of the values of the parameters, which means that this fixed point is unattainable.

The fixed point $\left(0, \frac{c_1}{c_2}\right)$ represents the case where cancer expands to full capacity and the cancer-reactive T cells die off completely. This is the most undesirable state, and we will later show that the fixed point is *unstable* for biologically reasonable parameter choices.

The final fixed point, $\left(\frac{c_1 - c_2 b_1/b}{c_3}, \frac{b_1}{b}\right)$, represents the scenario where the cancer and T cell populations coexist at relatively low populations. This means that cancer is not completely eliminated, but is controlled by the immune response. For biologically reasonable parameters, we will show that this fixed point can be *stable* for appropriate values of the delays.

To study the stability of (3), we linearize it around a fixed point (T_0, C_0) and obtain

$$\begin{cases} \frac{dT(t)}{dt} = -\tilde{b}_1 T(t) - b_2 T_0 C(t) \\ \qquad\quad +b_3 C_0 T(t-\sigma) + b_3 T_0 C(t-\sigma) \\ \qquad\quad +b_4 C_0 T(t-\tilde{\tau}) + b_4 T_0 C(t-\tilde{\tau}) \\ \qquad\quad +b_5 C_0 T(t-\tilde{\upsilon}) + b_5 T_0 C(t-\tilde{\upsilon}), \\ \frac{dC(t)}{dt} = \tilde{c}_1 C(t) - c_3 C_0 T(t-\rho) - c_3 T_0 C(t-\rho), \end{cases} \tag{4}$$

where $\tilde{b}_1 = b_1 + b_2 C_0$ and $\tilde{c}_1 = c_1 - 2c_2 C_0$.

A. Stability analysis without delays

The first step in studying the stability of the fixed points of (4) is to study the stability when all delays are set to zero, i.e.,

$$\begin{cases} \frac{dT(t)}{dt} &= (-b_1 + b C_0) T(t) + b T_0 C(t), \\ \frac{dC(t)}{dt} &= -c_3 C_0 T(t) + (\tilde{c}_1 - c_3 T_0) C(t). \end{cases} \tag{5}$$

The characteristic equation of (5) is

$$\det \begin{bmatrix} -b_1 + b C_0 - s & b T_0 \\ -c_3 C_0 & \tilde{c}_1 - c_3 T_0 - s \end{bmatrix},$$

which simplifies to

$$s^2 + (b_1 - \tilde{c}_1 - b C_0 + c_3 T_0) s + (-b_1 \tilde{c}_1 + b_1 c_3 T_0 + b \tilde{c}_1 C_0) = 0.$$

In conclusion, we have the following fixed points:

1) Fixed point I (FP–I): $(T_0, C_0) = (0,0)$.
   In this case, the characteristic equation is
   $$s^2 + (b_1 - \tilde{c}_1) s - b_1 \tilde{c}_1 = (s + b_1)(s - \tilde{c}_1),$$
   which means that the stability of FP–I is a *saddle*, since $b_1 \tilde{c}_1 = b_1 c_1$ is always a positive quantity.
2) Fixed point II (FP–II): $(T_0, C_0) = (0, c_1/c_2)$.
   Here, the characteristic equation is
   $$s^2 + (b_1 - \tilde{c}_1 - b c_1/c_2) s + (-b_1 \tilde{c}_1 + b \tilde{c}_1 c_1/c_2). \tag{6}$$
   Recall that $\tilde{c}_1 = c_1 - 2c_2 C_0 = c_1 - 2c_1 = -c_1$, so (6) simplifies to
   $$s^2 + (b_1 + c_1 - b c_1/c_2) s + (b_1 c_1 - b c_1^2/c_2). \tag{7}$$
   The discriminant of (7) is
   $$D = \left(b_1 - c_1 - \frac{b c_1}{c_2}\right)^2. \tag{8}$$
   Hence, the stability of FP–II depends on the parameters.

3) Fixed point III (FP–III): $(T_0, C_0) = \left(\frac{c_1 - c_2 b_1/b}{c_3}, \frac{b_1}{b}\right)$. In this case the characteristic equation is

$$s^2 + \frac{b_1 c_2}{b} s + b_1 \left(c_1 - \frac{b_1 c_2}{b}\right). \quad (9)$$

The discriminant of (9) is

$$D = \left(\frac{b_1 c_2}{b}\right)^2 - 4 b_1 \left(c_1 - \frac{b_1 c_2}{b}\right). \quad (10)$$

Similar to FP–II, the stability of FP–III depends on the parameters.

Notice that the parameters considered in [7] define FP–II and FP–III as an *unstable*, and respectively *stable* fixed points. Further discussions are included in Section IV.

B. Linearized model structure in presence of delays

The characteristic equation of (4) is $\det(sI - A(e^{-s})) = 0$, where

$$\begin{aligned}
A_{11}(e^{-s}) &= \tilde{b}_1 - b_3 C_0 e^{-\sigma s} - b_4 C_0 e^{-\tilde{\tau} s} - b_5 C_0 e^{-\tilde{\upsilon} s},\\
A_{12}(e^{-s}) &= -b_2 T_0 + b_3 T_0 e^{-\sigma s} + b_4 T_0 e^{-\tilde{\tau} s} + b_5 T_0 e^{-\tilde{\upsilon} s},\\
A_{21}(e^{-s}) &= -c_3 C_0 e^{-\rho s},\\
A_{22}(e^{-s}) &= \tilde{c}_1 - c_3 T_0 e^{-\rho s}.
\end{aligned}$$

It is important to note that the characteristic equation (4) has a particular structure since the corresponding "entry" matrices for the delays ρ, $\tilde{\tau}$, $\tilde{\upsilon}$, and σ are of *rank one*, which simplifies the characteristic equation. More precisely, the characteristic equation writes as follows:

$$\begin{aligned}
p_0(s) + p_1(s) e^{-\rho s} + p_2(s) e^{-\sigma s} + p_3(s) e^{-\tilde{\tau} s}\\
+ p_4(s) e^{-\tilde{\upsilon} s} = 0,
\end{aligned}$$

where

$$\begin{aligned}
p_0(s) &= -(\tilde{b}_1 + s)(\tilde{c}_1 - s),\\
p_1(s) &= c_3 T_0 (b_1 + s),\\
p_2(s) &= b_3 C_0 (\tilde{c}_1 - s),\\
p_3(s) &= b_4 C_0 (\tilde{c}_1 - s),\\
p_4(s) &= b_5 C_0 (\tilde{c}_1 - s).
\end{aligned}$$

Since $p_0(s)$ has no purely imaginary roots, we write

$$\begin{aligned}
a(s) = 1 + a_1(s) e^{-\rho s} + a_2(s) e^{-\sigma s} + a_3(s) e^{-\tilde{\tau} s}\\
+ a_4(s) e^{-\tilde{\upsilon} s}, \quad (11)
\end{aligned}$$

where $a_k(s) = p_k(s)/p_0(s)$.

III. Main results

One way of visualizing the crossing surface of (4) is to fix two delays and determine the crossing curves for the other two delays. Based on the particular form of the characteristic equation and of the delays scales, it seems reasonable to consider the (natural) delays *partition* in *small*, and *large* delays.

Introduce now an *auxiliary system* associated to small delays, and given by the following characteristic equation:

$$a_{\rho,\sigma}(s) \quad = \quad 1 + a_1(s) e^{-\rho s} + a_2(s) e^{-\sigma s} = 0. \quad (12)$$

Using the *geometric approach* proposed by [10], we can easily characterize the *stability crossing curves* of $a_{\rho,\sigma}(s)$ given by (12) in the delay-parameter space defined by the small delays ρ, and σ. Based on such a characterization, and using a standard continuity argument (see, for instance, [6]) of the roots of the characteristic equation (11) with respect to the delay parameters, we make the following assumption:

Assumption 1: Let $\mathcal{I}_\rho \subset \mathbb{R}_+$, and $\mathcal{I}_\sigma \subset \mathbb{R}_+$ be some real intervals such that there exists some $\delta > 0$, such that $a_{\rho,\sigma}(s) \neq 0$ for all the pairs $(\sigma, \rho) \in \mathcal{I}_\sigma \times \mathcal{I}_\rho$, and for all $s \in \mathcal{V}_\delta$, where $\mathcal{V}_\delta$ is defined by:

$$\mathcal{V}_\delta \quad = \quad \{s \in \mathbb{C} : \quad -\delta < Re(s) < \delta\}. \quad (13)$$

The assumption above can be seen as a *regularity* condition for the original linearized model, and it simply says that there exists some delay intervals such that $a_{\rho,\sigma}$ is *invertible* in some neighborhood $\mathcal{V}_\delta$ of the imaginary axis for all the pairs $(\sigma, \rho) \in \mathcal{I}_\sigma \times \mathcal{I}_\rho$.

It is important to note that the assumption above is not restrictive. Indeed, assume now that there exists at least one root on the imaginary axis for the auxiliary characteristic equation $a_{\rho,\sigma}(s) = 0$. Then the number of roots on the imaginary axis of $a_{\rho,\sigma}(s) = 0$ is always *finite* (see the arguments in [10]).

Next, if $j\omega_c \neq 0$ is one of such roots of the auxiliary characteristic equation $a_{\rho,\sigma}(j\omega_c) = 0$, than it is also a root of (11) *if and only if* $\mid p_3(j\omega_c) \mid = \mid p_4(j\omega_c)$. If not, the regularity condition $a_{\sigma,\rho}(s) \neq 0$ is *still* valid on some interval on the imaginary axis $\mathcal{I}_\omega$ including $j\omega_c$.

A. Identification of the crossing points, and crossing set characterization

We have the following result:

Proposition 2: Assume that the auxiliary system given by (12) satisfies the Assumption 1. Define now $a_{\tilde{\tau},\tilde{\upsilon}}$ by:

$$a_{\tilde{\tau},\tilde{\upsilon}}(s) \quad = \quad 1 + a_{\tilde{\tau}}(s) e^{-s\tilde{\tau}} + a_{\tilde{\upsilon}}(s) e^{-s\tilde{\upsilon}}, \quad (14)$$

where:

$$a_{\tilde{\tau}}(s) = \frac{p_3(s)}{a_{\sigma,\rho}(s)}, \qquad a_{\tilde{\upsilon}}(s) = \frac{p_4(s)}{a_{\sigma,\rho}(s)},$$

for all $(\sigma, \rho) \in \mathcal{I}_\sigma \times \mathcal{I}_\rho$. Then for any $(\sigma, \rho) \in \mathcal{I}_\sigma \times \mathcal{I}_\rho$, the characteristic equation associated to (11) and $a_{\tilde{\tau},\tilde{\upsilon}}(s)$ have the same solutions in a neighborhood $\mathcal{V}_\delta$ of the imaginary axis, where:

$$\mathcal{V}_\delta = \{s \in \mathbb{C} : \quad \delta \geq Re(s) > -\delta\},$$

for some $\delta > 0$.

Proof. The proof follows from the continuity argument with respect to the delay parameters (see, e.g. [6]), and from the equivalence between the characteristic equations (14) and (11) if $a_{\rho,\sigma}(s) \neq 0$ in some vertical strip including the imaginary axis (Assumption 1). □

B. Weak T/C interactions, and delay-independence type results

As mentioned in the Introduction, we will consider first the case of *weak T/C cell interactions*. Without any loss of generality, a weak T/C interaction simply means a reduced probability of interactions of anti-cancer and cancer cells. In other words, the weak T/C interaction describes the situations when the anti-cancer cells will "mostly" "ignore" the cancer cells. Roughly speaking, such a T/C interaction will be translated in "small" values for $b_4 = 2^N p_1 q_1 k$, and $b_5 = p_1 q_2 k$, which may correspond to the case when *no crossing* in the delay-parameter space defined by large delays exists. In conclusion, a weak T/C interaction may correspond to some *delay-independent* type property with respect to the delay parameters under consideration, and the last argument will give a way to define a *measure* for characterizing the interaction character.

With the notations, and the results above, we have the following:

Proposition 3 (Delay-independence in large delays): Assume that the auxiliary system given by the characteristic equation (12) satisfies the Assumption 1, and that $a_{\tilde{\tau},\tilde{\upsilon}}(0) \neq 0$, where $a_{\tilde{\tau},\tilde{\upsilon}}$ is defined by (14).

Then the following statements are equivalent:

(a) If the auxiliary system (12) is stable for some pair $(\rho, \sigma) \in \mathcal{I}_\rho \times \mathcal{I}_\sigma$, and if the system free of delays ($\sigma = \rho = \mu = \upsilon \equiv 0$) given by (5) is stable, then the system (3) is stable for all pairs $(\tilde{\tau}, \tilde{\upsilon}) \in \mathbb{R}_+ \times \mathbb{R}_+$, and there does not exist any root crossing the imaginary axis when the delays $\tilde{\tau}$, and $\tilde{\upsilon}$ are increased in $\mathbb{R}_+$.

(b) The following frequency-sweeping test holds:

$$\frac{\mid C_0 \mid \sqrt{\tilde{c}_1^2 + \omega^2}}{\mid a_{\tilde{\tau},\tilde{\upsilon}}(j\omega) \mid} < \frac{1}{(2^N q_1 + q_2) p_1 k}, \quad \forall \omega > 0. \quad (15)$$

The same equivalence holds if the stability property is replaced by the instability of the system with a prescribed number of unstable roots.

Proof. It is easy to see that the condition (15) is equivalent to the condition $a_{\tilde{\tau},\tilde{\upsilon}}(j\omega) \neq 0$, for all $\omega > 0$. Then the equivalence between conditions *(a)* and *(b)* above follows straightforwardly since $a_{\tilde{\tau},\tilde{\upsilon}} \neq 0$ whenever $\omega = 0$ (see, for instance, the arguments in [9], [19] for delay-independent stability characterization). □

In other words, the result above gives a simple test for describing the situations when the system (3), *stable* or *unstable* in the case when is *delay-free*, will remain *stable* or respectively *unstable* for *all positive (large) delays* $\tilde{\tau}$, and $\tilde{\upsilon}$.

Remark 4: The main difference between the result above, and the standard *delay-independent* frequency-sweeping tests (see, e.g. [9]) is given by the fact that, in our case, we do not impose the delay-independent property with respect to the *whole* set of delays, that is: ρ, σ, $\tilde{\upsilon}$, and $\tilde{\tau}$, but only on some *partition* of it: delay-independent with respect to $\tilde{\tau}$, and $\tilde{\upsilon}$. Several remarks about "mixed" delay-independent/delay-dependent stability results can be found in [19]. Furthermore, the *delay-independent* character can be seen as the existence of at least one *unbounded* direction in the corresponding delay-parameter set.

Remark 5 (Weak T/C interaction measure): The frequency-sweeping test (15) can be used to define a measure for characterizing the T/C interaction type in the following sense: the T/C interaction will be called *weak* if the probabilities (q_1, q_2), and the average number of cell division N verify the condition:

$$2^N q_1 + q_2 \quad < \quad \frac{1}{p_1 k} \cdot \frac{1}{\sup_{\omega \in \mathbb{R}} \frac{|C_0| \sqrt{\tilde{c}_1^2 + \omega^2}}{|a_{\tilde{\tau},\tilde{\upsilon}}(j\omega)|}}. \quad (16)$$

The condition (16) gives the corresponding *T/C interaction measure*. It becomes clear that the average number N of cell division plays a central role in defining the T/C interaction character, since the quantity $2^N q_1 + q_2$ is an increasing function of N.

C. Strong T/C interactions, and identification of the crossing points

As mentioned in the previous paragraph, the existence of crossing sets in the delay-parameter space defined by $\tilde{\tau}$ and $\tilde{\upsilon}$ is related to the fact that the inequality (15) is not verified for all $\omega > 0$, or in other words that the parameters (q_1, q_2, N) do not satisfy the measure condition (16) for the T/C weak interaction.

Inspired by the work in [10], the condition that $a_{\tilde{\tau},\tilde{\upsilon}}$ defined by (14) has at least one root $j\omega_0$ on the imaginary axis is reduced geometrically to the condition that the "lengths" 1, $\mid a_\upsilon(j\omega_0) \mid$, and $\mid a_\mu(j\omega_0) \mid$ define a triangle. Thus, some simple computations lead to the following criterion for the *identification of the crossing points*:

Proposition 6: Assume that the auxiliary system given by the characteristic equation (12) satisfies the Assumption 1. Then each $\omega \in \mathbb{R}_+$ can be a solution of the characteristic equation associated to Σ for some $(\tilde{\tau}, \tilde{\upsilon}) \in \mathbb{R}_+^2$ if and only if:

$$\frac{1}{(2^N q_1 + q_2) p_1 k} \leq \frac{\mid C_0 \mid \sqrt{\tilde{c}_1^2 + \omega^2}}{\mid a_{\tilde{\tau},\tilde{\upsilon}}(j\omega) \mid} \leq \frac{1}{\mid 2^N q_1 - q_2 \mid p_1 k}. \quad (17)$$

Then, the *crossing set* Ω will be defined by all $\omega \in \mathbb{R}_+$, for which the frequency condition (17) holds. In conclusion, the algorithm for identifying the crossing points can be resumed as follows:

- first, we represent graphically $\dfrac{\mid C_0 \mid \sqrt{\tilde{c}_1^2 + \omega^2}}{\mid a_{\tilde{\tau},\tilde{\upsilon}}(j\omega) \mid}$ against ω, and
- next we analyse the intersection of this graphic with two parallel lines to ω-axis: $1/((2^N q_1 + q_2) p_1 k)$ and $1/(\mid 2^N q_1 - q_2 \mid p_1 k)$, respectively.

Let $\omega \in \Omega$ be a crossing point. Then from the triangle

geometry it follows that:

$$\tilde{\tau} = \tilde{\tau}^{u\pm}(\omega) = \frac{\angle a_{\tilde{\tau}}(j\omega) + (2u-1)\pi \pm \theta_1}{\omega} \geq 0, \quad u = u_0^{\pm}, u_0^{\pm}+1, u_0^{\pm}+2, ..., \tag{18}$$

$$\tilde{\upsilon} = \tilde{\upsilon}^{v\pm}(\omega) = \frac{\angle a_{\tilde{\upsilon}}(j\omega) + (2v-1)\pi \mp \theta_2}{\omega} \geq 0, \quad v = v_0^{\pm}, v_0^{\pm}+1, v_0^{\pm}+2, ..., \tag{19}$$

where $\theta_1, \theta_2 \in [0, \pi]$ are the internal angles of the triangle formed by the lengths 1, $\mid a_\mu \mid$, and $\mid a_\upsilon \mid$, and can be calculated by the law of cosine as

$$\theta_1 = \cos^{-1}\left(\frac{1+|a_{\tilde{\tau}}(j\omega)|^2 - |a_{\tilde{\upsilon}}(j\omega)|^2}{2|a_{\tilde{\tau}}(j\omega)|}\right), \tag{20}$$

$$\theta_2 = \cos^{-1}\left(\frac{1+|a_{\tilde{\upsilon}}(j\omega)|^2 - |a_{\tilde{\tau}}(j\omega)|^2}{2|a_{\tilde{\upsilon}}(j\omega)|}\right), \tag{21}$$

and u_0^+, u_0^-, v_0^+, v_0^- are the smallest possible integers (may be negative and may depend on ω) such that the corresponding $\mu^{u_0^+ +}$, $\mu^{u_0^- -}$, $\upsilon^{v_0^+ +}$, $\upsilon^{v_0^- -}$ calculated are nonnegative.

Let $\mathcal{T}^+_{\omega,u,v}$ and $\mathcal{T}^-_{\omega,u,v}$ be the singletons defined by

$$\mathcal{T}^{\pm}_{\omega,u,v} = \{(\tau_1^{u\pm}(\omega), \tau_2^{v\pm}(\omega))\},$$

and define

$$\mathcal{T}_\omega = \left(\bigcup_{\substack{u\geq u_0^+ \\ v\geq v_0^+}} \mathcal{T}^+_{\omega,u,v}\right) \bigcup \left(\bigcup_{\substack{u\geq u_0^- \\ v\geq v_0^-}} \mathcal{T}^-_{\omega,u,v}\right).$$

Then $\mathcal{T}_\omega$ is the set of all (μ, υ) such that $a_{\tilde{\tau},\tilde{\upsilon}}$ has one zero at $s = j\omega$.

Remark 7: It is easy to see that $\dfrac{\mid C_0 \mid \sqrt{\tilde{c}_1^2 + \omega^2}}{\mid a_{\tilde{\tau},\tilde{\upsilon}}(j\omega) \mid} \to 0$, when $\omega \to +\infty$, and in conclusion $\infty \notin \Omega$. In other words, Ω is *bounded*.

D. Characterization of the crossing curves

The next step is to characterize the crossing curves of the system (3), or equivalently all the crossing curves satisfying $a_{\tilde{\tau},\tilde{\upsilon}}(s) = 0$ for $s = j\omega$, $\omega \in \Omega$.

Using an argument similar to the one developed by [10] (type classification of the crossing points), define by $\Omega_k \subset \Omega$ some interval of crossing set Ω, and let $\mathcal{T}^k \subset \mathcal{T}$ be the corresponding stability crossing curves for some positive integer k, we have the following:

Proposition 8: Under the standing assumption (1), the stability crossing curves $\mathcal{T}^k$ corresponding to Ω_k must be an intersection of $\mathbb{R}^2_+$ with a series of curves belonging to one of the following categories:

A. A series of closed curves;

B. A series of spiral-like curves with axes oriented either horizontally, vertically, or diagonally.

C. A series of open ended curves with both ends approaching ∞.

Remark 9: The classification above is given by the way the end points of the corresponding intervals Ω_k are derived.

E. Tangent and smoothness

In this section, for a given k, we will discuss the smoothness of the curves in $\mathcal{T}^k$ and thus $\mathcal{T} = \bigcup_{k=1}^{N} \mathcal{T}^k$. We will understand a k is given and will refer to $\mathcal{T}^k$ without further comments. In addition to the explicit formulas (18) and (19), we will also use an approach similar to the one described in Chapter 11 of [8] based on the implicit function theorem.

For this purpose, we consider $\tilde{\tau}$ and $\tilde{\upsilon}$ as implicit functions of $s = j\omega$ defined by $a_{\tilde{\tau},\tilde{\upsilon}} = 0$. As s moves along the imaginary axis, $(\tilde{\tau},\ \tilde{\upsilon}) = (\tilde{\tau}^{u\pm}(\omega), \tilde{\upsilon}^{v\pm}(\omega))$ moves along $\mathcal{T}^k$.

For a given $\omega \in \Omega_k$, let

$$R_0 = Re\left(\frac{j}{s}\frac{\partial a_{\tilde{\tau},\tilde{\upsilon}}(s)}{\partial s}\right)_{s=j\omega} = \frac{1}{\omega} Re\left(\left[a'_{\tilde{\tau}}(j\omega) - \tilde{\tau} a_{\tilde{\tau}}(j\omega)\right] e^{-j\tilde{\tau}\omega} + [a'_{\tilde{\upsilon}}(j\omega) - \tilde{\upsilon} a_{\tilde{\upsilon}}(j\omega)] e^{-j\tilde{\upsilon}\omega}\right), \tag{22}$$

$$I_0 = Im\left(\frac{j}{s}\frac{\partial a_{\tilde{\tau},\tilde{\upsilon}}(s)}{\partial s}\right)_{s=j\omega} = \frac{1}{\omega} Im\left(\left[a'_{\tilde{\tau}}(j\omega) - \tilde{\tau} a_{\tilde{\tau}}(j\omega)\right] e^{-j\tilde{\tau}\omega} + [a'_{\tilde{\upsilon}}(j\omega) - \tilde{\upsilon} a_{\tilde{\upsilon}}(j\omega)] e^{-j\tilde{\upsilon}\omega}\right), \tag{23}$$

and

$$R_l = -Re\left(\frac{1}{s}\frac{\partial a_{\tilde{\tau},\tilde{\upsilon}}(s))}{\partial \tau_k}\right)_{s=j\omega}, \tag{24}$$

$$I_l = -Im\left(\frac{1}{s}\frac{\partial a_{\tilde{\tau},\tilde{\upsilon}}(s)}{\partial \tau_k}\right)_{s=j\omega}, \tag{25}$$

for $l = 1, 2$, and τ_1, τ_2 correspond to $\tilde{\tau}$, and $\tilde{\upsilon}$, respectively. Then, since $a_{\tilde{\tau},\tilde{\upsilon}}(s)$ is an analytic function of s, $\tilde{\tau}$ and $\tilde{\upsilon}$, the implicit function theorem indicates that the tangent of $\mathcal{T}^k$ can be expressed as

$$\begin{pmatrix} \frac{d\mu}{d\omega} \\ \frac{d\upsilon}{d\omega} \end{pmatrix} = \begin{pmatrix} R_1 & R_2 \\ I_1 & I_2 \end{pmatrix}^{-1} \begin{pmatrix} R_0 \\ I_0 \end{pmatrix} = \frac{1}{R_1 I_2 - R_2 I_1} \begin{pmatrix} R_0 I_2 - I_0 R_2 \\ I_0 R_1 - R_0 I_1 \end{pmatrix}, \tag{26}$$

provided that

$$R_1 I_2 - R_2 I_1 \neq 0. \tag{27}$$

It follows from a well known result [3] that $\mathcal{T}^k$ is smooth everywhere except possibly at the points where either (27) is not satisfied, or when

$$\frac{d\tau_1}{d\omega} = \frac{d\tau_2}{d\omega} = 0. \tag{28}$$

A careful examination of these cases allows us concluding that

Proposition 10: Under the standing assumptions including (1), the curves in $\mathcal{T}^k$ are smooth everywhere except possibly at the degenerate points corresponding to ω in any one of the following two cases:

Case 1. $s = j\omega$ is a multiple solution of $q_{\mu,\upsilon}(j\omega, e^{-j\omega}) = 0$.

Case 2. ω is an end point, and $\frac{d}{d\omega}(|g(j\omega, \rho, \sigma)|) = 0$.

F. Direction of crossing

Next, we will discuss the direction in which the solutions of the characteristic equation given by $a_{\tilde{\tau},\tilde{\upsilon}}(s) = 0$ cross the imaginary axis as $(\tilde{\tau}, \tilde{\upsilon})$ deviates from a curve in $\mathcal{T}^k$. We will call the direction of the curve that corresponds to increasing ω the *positive direction*. Notice, as the curve passes through the points corresponding to the end points of Ω_k, the positive direction is reversed. We will also call the region on the left hand side as we head in the positive direction of the curve *the region on the left*. Again, due to the possible reversion of parametrization, the same region may be considered on the left with respect to one point of the curve, and be considered as on the right on another point of the curve.

For the purpose of discussing the direction of crossing, we need to consider $\tilde{\tau}$ and $\tilde{\upsilon}$ as functions of $s = r + j\omega$, i.e., functions of two real variables r and ω, and partial derivative notation needs to be adopted instead. Since the tangent of $\mathcal{T}^k$ along the positive direction is $(\partial\tilde{\tau}/\partial\omega, \partial\tilde{\upsilon}/\partial\omega)$, the normal to $\mathcal{T}^k$ pointing to the left hand side of the positive direction is $(-\partial\tilde{\upsilon}/\partial\omega, \partial\tilde{\tau}/\partial\omega)$. Also, as a pair of complex conjugate solutions of $a_{\tilde{\tau},\tilde{\upsilon}} = 0$ cross the imaginary axis to the $\mathbb{C}_+$, $(\tilde{\tau}, \tilde{\upsilon})$ move along the direction $(\partial\tilde{\tau}/\partial r, \partial\tilde{\upsilon}/\partial r)$. We can therefore conclude that if the inner product of these two vectors are positive, i.e.,

$$\left[\frac{\partial\tilde{\tau}}{\partial\omega}\frac{\partial\tilde{\upsilon}}{\partial r} - \frac{\partial\tilde{\upsilon}}{\partial\omega}\frac{\partial\tilde{\tau}}{\partial r}\right]_{s=j\omega} > 0, \tag{29}$$

the region on the left of $\mathcal{T}^k$ at ω has two more solutions in $\mathbb{C}_+$. On the other hand, if the inequality in (29) is reversed, then the region on the left of $\mathcal{T}^k$ has two fewer solutions on the right hand side of the complex plane. We can very easily express, parallel to (26), that,

$$\begin{aligned}\begin{pmatrix} \frac{\partial\tilde{\tau}}{\partial r} \\ \frac{\partial\tilde{\upsilon}}{\partial r} \end{pmatrix}_{s=j\omega} &= \begin{pmatrix} R_1 & R_2 \\ I_1 & I_2 \end{pmatrix}^{-1} \begin{pmatrix} I_0 \\ -R_0 \end{pmatrix} \\ &= \frac{1}{R_1 I_2 - R_2 I_1} \begin{pmatrix} R_0 R_2 + I_0 I_2 \\ -R_0 R_1 - I_0 I_1 \end{pmatrix}, \end{aligned} \tag{30}$$

where R_l and I_l, $l = 0, 1, 2$, are defined in (22) to (25). This allows us to arrive at the following proposition.

Proposition 11: Let $\omega \in \Omega_k$, but an end point, and $(\tilde{\tau}, \tilde{\upsilon}) \in \mathcal{T}^k$ such that $j\omega$ is a simple solution of $a_{\tilde{\tau},\tilde{\upsilon}}(s) = 0$, and

$$a_{\tilde{\tau},\tilde{\upsilon}}(j\omega') \neq 0, \text{ for any } \omega' > 0,\ \omega' \neq \omega. \tag{31}$$

Then as $(\tilde{\tau}, \tilde{\upsilon})$ moves from the region on the right to the the region on the left of the corresponding curve in $\mathcal{T}^k$, a pair of solutions of $a_{\tilde{\tau},\tilde{\upsilon}}(s) = 0$ cross the imaginary axis to the right if

$$R_2 I_1 - R_1 I_2 > 0. \tag{32}$$

The crossing is in the opposite direction if the inequality is reversed.

IV. Illustrative example

In this section, we show how the techniques developed in Sections 3 and 4 can be used to study the stability in the delay space of model (1). The analysis is completed by various discussions on the results derived together with their interpretations.

A. Stability without delays

For our application in [7], we estimated values of the parameters to be approximately

$$\begin{array}{lll} d_T = 0.2, & p_1 = 0.5, & \rho = 0.0035, \\ r = 0.2, & p_2 = 0.5, & \sigma = 0.0007, \\ k = 1, & q_1 = 0.5, & \tilde{\tau} = 2.0035, \\ N = 2, & q_2 = 0.5, & \tilde{\upsilon} = 1.0035. \\ K = 200, & \tilde{p}_1 = 0.5, & \end{array} \tag{33}$$

Hence, b_1, c_1, and b are of order 1 or 0.1, while $c_1/c_2 = K$, the carrying capacity of the cancer population, which is around 200.

Proposition 12: The fixed points of the linearized system without delay have the following properties:

(a) The fixed-point FP-I $(T_0, C_O) = (0, 0)$ is a saddle.
(b) The fixed point FP-II $(T_0, C_0) = (0, c_1/c_2)$ is unstable.
(c) The fixed point FP-III $(T_0, C_0) = \left(\frac{c_1 - c_2 b_1/b}{c_3}, \frac{b_1}{b}\right)$ is stable.

Proof. (a) As mentioned in Section II, FP–I is a saddle independently of the parameters' choice. (b) Next, for the considered parameters, simple computations prove that the discriminant (8) and the middle term of (7) are both negative, making the fixed point FP-II an unstable spiral. (c) In this case, for parameters in the vicinity of (33), the first term of (10) is of order $1/K^2 \sim 10^{-4}$ and the second term is an order 10^{-1}, so the discriminant is of order -10^{-1}. Thus, the solution at the controlled disease fixed point is a stable spiral. □

In our case, FP–III is of *most interest* to us because it is stable and represents the case where the immune response controls the cancer population. However, since the middle term of (9) is $b_1 c_2/b \sim 10^{-4}$, the approach to the fixed point is very slow. In fact, the stability of the fixed point is so low that numerical error may cause the solution to become unstable. When solving DDEs in Matlab, one way around this problem is to increase the relative and absolute tolerances of the MATLAB DDE solver.

B. Stability with delays

As mentioned in the previous section, one way of visualizing the crossing surface of (4) is to fix two delays and determine the crossing curves for the other two delays. This procedure is demonstrated in Figure 3.

In this case, any pairwise combination of ρ, σ, or τ gives open curves such as the ones shown on the left side of Figure 3. Any pair containing υ leads to spiral-like curves such as the ones shown on the right side of Figure 3.

For the choice of parameters in (33), fixed point III is stable in the no-delay case, so there is a stability region for sufficiently small delays. However, this region is very small and disappears quickly as the delays increase. Figure 4 shows the crossing curves for σ vs. ρ, when $(\tau, \upsilon) = (0, 0)$ for the linearization of (3) around fixed point III, $\left(\frac{c_1 - c_2 b_1/b}{c_3}, \frac{b_1}{b}\right)$.

In particular, the delays for T cell division, $\tilde{\tau}$, and recovery from a cytotoxic process, $\tilde{\upsilon}$, are about 2 and 1 days, respectively, so fixed point III is unstable.

However, for low values of ρ and σ, we find another stable region in $(\tilde{\tau}, \tilde{\upsilon})$-space away from the origin. For $\rho = 0.0035$ and $\sigma = 0.0007$, the crossing curves for $\tilde{\tau}$ and $\tilde{\upsilon}$ are shown in Figure 5(left). A stable solution is shown in Figure 5(right).

In this region, the values for ρ and σ are 5 and 1 minutes as estimated in (33). The delay $\tilde{\tau}$, corresponding to $N = 2$ cell divisions, is about 1 day, which is a little fast, but still reasonable. On the other hand, the delay $\tilde{\upsilon}$, corresponding to the turn around time for T cell recovery after cytotoxic responses, is around 20 to 30 days, which is far longer than the expected 1 day turn around time.

From the perspective of medical intervention, the larger stable region away from the origin is more interesting, because it is probably easier to slow rates down than to speed them up. For contrast, consider the small stable region around the origin in Figure 5. In this region, the delays $\tilde{\tau}$ and $\tilde{\upsilon}$ are constrained to values less than 0.005 (7 min) and 0.02 (30 min), respectively, and it is almost impossible to accelerate T cell division or the T cell recovery time to these rates.

C. Stabilization by changing non-delay parameters

Because of the interdependence of the non-delay parameters, it is difficult (but not impossible) to generate crossing diagrams for each of the parameters. As a result, we study numerically the effect of non-delay parameters on stability. As before, we focus on the stability of fixed point III.

For most parameters, the stability region around the origin is very small, so we approximate the region as a 4-dimensional polyhedron with planar faces. Furthermore, it is straightforward to calculate the values of the points on the ρ, σ, $\tilde{\tau}$, and $\tilde{\upsilon}$ axes that bound this polyhedron. These calculations entail solving the caracteristic equation (9) for one delay, while setting the other delays to 0. The expressions for these values are given in Appendix . If the values of these points are sufficiently small, the volume of the stable region is close to the volume of the polyhedron defined by the four points and the origin. This approximation is no longer useful if the volume of the polyhedron is large or if a point does not exist, i.e., if the crossing surface no longer intersects one of the axes.

We vary the non-delay parameters according to the ranges shown in Table I and calculate the volume of the polyhedron for all combinations of these values. Average polyhedron volumes for individual parameter values are shown in Figure 6. In these figures, we plot the volume obtained by fixing one parameter and averaging over the volumes obtained by varying the other parameters.

The parameters that influence the size of the stability region the most are the kinetic coefficient k and the T cell death rate d_T. Lower kinetic rates k and higher T cell death rates d_T lead to larger stable regions. In either case, the region around the origin is not large enough to allow for biologically meaningful values of $\tilde{\tau}$ and $\tilde{\upsilon}$.

However, if we consider the extreme case where we set $k = 0.01$, $d_T = 0.5$, all other parameters according to the estimates in (33), and $(\rho, \sigma) = (0.0035, 0.0007)$, we obtain the stable region shown in Figure 7.

Here, the assumption that the stable region is approximated by a polyhedron collapses, so the numerical analysis discussed above is invalid. However, this region covers a large area in $(\tilde{\tau}, \tilde{\upsilon})$-space, including the biologically reasonable point $(\tilde{\tau}, \tilde{\upsilon}) = (2, 1)$.

D. Discussion

Surprisingly, the results indicate that the stability of the controlled state, fixed point III, benefits from T cells that are slowly reacting, rapidly dying, and have long turn around times after killing cancer cells. These results are counterintuitive.

While, in principle, we cannot overrule such results from being biologically significant, it is probably reasonale to assume that our model is too simple to capture the full nature of the interactions. Specifically, the delay term corresponding to ρ in (3) causes the cancer population to sometimes pass below zero. This, in turn, drags the T cell population below zero and often results in an unstable oscillation. This situation is unrealistic, and as a result, stability usually entails avoiding these situations. More inert T cells lead to more gradual declines of the cancer populations, which reduce the likelihood that either population swings very much below zero. Hence, in this formulation of the CML model, more gradual reduction of the cancer population is favored over rapid elimination. We did not have to deal with this issue in our previous CML work, [7], since there we studied the ruin problem, i.e., once the cancer population hit zero, we stopped.

It is straightforward to reformulate the model so that neither population can pass below zero. The study of such a model is left for future work.

V. Concluding remarks

This paper addressed the problem of characterization of stability boundaries in some delay-parameter set for a dynamical system including *four* (independent) *delays*, system that describes the post-transplantation dynamics of the immune response to chronic myelogenous leukemia. Such a model includes two small delays, and two large delays.

The stability analysis proposed in the paper allowed us to define two types of T/C cell interactions: weak, and strong, and a quantitative measure for the weak T/C interaction was introduced, and explicitly computed.

Furthermore, we have proved that the large delay values have a low influence on the stability properties in the weak cell interaction case. Next, the strong cell interaction case was analyzed in terms of stability crossing curves, and a classification of the such crossing curves is given. Finally, an example was considered for illustrating the derived results. Several interpretations and discussions complete the presentation.

REFERENCES

[1] Beretta, E. and Kuang, Y.: Geometric stability switch criteria in delay differential systems with delay dependent parameters. *SIAM J. Math. Anal.* **33** (2002) 1144-1165.

[2] Boese, F.G.: Stability with respect to the delay: On the paper of K.L. Cooke and P. van den Driessche. *J. Math. Anal.Appl.*, **228** (1998) 293-321.

[3] Bruce, J.W., and Giblin, P.J.: *Curves and singularities* (Cambridge Univ. Press: Cambridge, 1984).

[4] Chao, D. L., Forrest, S., Davenport, M. P., Perelson, A. S.: Stochastic stage-structured modeling of the adaptive immune system. *Proc. of the Computational Systems Bioinformatics,* 2003.

[5] Cooke, K. L. and van den Driessche, P.: On zeroes of some transcendental equations. in *Funkcialaj Ekvacioj* **29** (1986) 77-90.

[6] Datko, R.: A procedure for determination of the exponential stability of certain differential-difference equations. *Quart. Appl. Math.* **36** (1978) 279-292.

[7] DeConde, R., Kim, P. S., Levy, D., Lee, P. P.: Post-transplantation dynamics of the immune response to chronic myelogenous leukemia. *J. Theor. Biol.* **236** (2005) 39-59.

[8] Diekmann, O., van Gils, S. A., Verduyn-Lunel, S. M. and Walther, H. -O.: *Delay equations, Functional-, Complex and Nonlinear Analysis* (Appl. Math. Sciences Series, **110**, Springer-Verlag, New York, 1995).

[9] Gu, K., Kharitonov, V.L. and Chen, J.: *Stability and robust stability of time-delay systems*. (Birkhauser: Boston, 2003).

[10] Gu, K., Niculescu, S.-I., and Chen, J.: On stability of crossing curves for general systems with two delays. in *J. Math. Anal. Appl.*, **311** (2005) 231-253.

[11] Hale, J. K. and Verduyn Lunel, S. M.: *Introduction to Functional Differential Equations* (Applied Math. Sciences, **99**, Springer-Verlag, New York, 1993).

[12] Kharitonov, V.L., Niculescu, S.-I., Moreno, J., and Michiels, W.: Stattic output feedback stabilization: Necessary conditions for multiple delay controllers. *IEEE Trans. Automat. Contr.*, **50** (2005) 82-86.

[13] Kim, P.S., DeConde, R., Levy, D., and Lee, P.: Post-transplantation dynamics of the immune response to chronic myelogenous leukemia. in presented at *Int. Conf. on Diff. Eqs. and Appli. in Math. Biology*, Nanaimo, BC, Canada, July 2004.

[14] Kuang, Y.: *Delay differential equations with applications in population dynamics* (Academic Press, Boston, 1993).

[15] MacDonald, N.: *Biological delay systems: linear stability theory*. (Cambridge University Press, Cambridge, 1989).

[16] Michiels, W., and Roose, D.: An eigenvalue based approach for the robust stabilization of linear time-delay systems. *Int. J. Control* **76** (2003) 678-686.

[17] Murray, J.D.: *Mathematical Biology* (BioMath. **18**, Springer: Berlin, 2nd Edition, 1993).

[18] Murali-Krishna, K., Altman, J. D., Suresh, M., Sourdive, D. J. D., Zajac, D. J. D., Miller, J. D., Slansky, J., Ahmed, R.: Counting antigen-specific CD8+ T cells: a re-evaluation of bystander activation during viral infection. *Immunity* **8** (1998) 177-187.

[19] Niculescu, S.-I.: *Delay effects on stability. A robust control approach* (Springer-Verlag: Heidelberg, LNCIS, vol. **269**, 2001).

[20] Niculescu, S.-I., Fu, P., and Chen, J.: Stability switches and reversals of linear systems with commensurate delays: A matrix pencil characterization. *Internal Note HeuDiaSyC'04* (submitted).

[21] Toker, O. and Özbay, H.: Complexity issues in robust stability of linear delay-differential systems. *Math., Contr., Signals, Syst.*, **9** (1996) 386-400.

[22] Walton, K., and Marshall, J.E.: Direct method for TDS stability analysis, *IEE Proceedings*, Pt. D, **134**(1987) 101-107.

APPENDIX

The ρ intercept, (i.e. the lowest non-negative point that a crossing surface intersects the ρ-axis in delay space), is

$$(\arctan(\omega/\tilde{c}_1) + \arctan(\omega/b_1) - \pi/2)/\omega,$$

where

$$\omega = \left(\frac{-B + \sqrt{B^2 - 4C}}{2}\right)^{1/2}, \tag{34}$$

and

$$B = \tilde{c}_1^2 - (c_1 - b_1c_2/b)^2, \qquad C = -b_1^2(c_1 - b_1c_2/b)^2.$$

The σ, $\tilde{\tau}$, and $\tilde{\upsilon}$ intercepts are of the form

$$\sigma = (-\arctan((\omega Q)/(\omega^2 + P)) - \arctan(\omega/\tilde{c}_1))/\omega,$$

where ω is as in (34) and

$$\begin{aligned} B &= 2P + Q^2 - R^2, \\ C &= P^2 - \tilde{c}_1^2 R^2, \\ P &= -b_1(c_1 - b_1c_2/b) + b_1b_i\tilde{c}_1/b, \\ Q &= \tilde{c}_1 - (c_1 - b_1c_2/b) - b_1b_i/b, \\ R &= b_1b_i/b, \end{aligned} \tag{35}$$

where $i = 3$, 4, and 5, respectively.

Param.	Description	Test values
d_T	T cell death rate	0.1, 0.12, 0.14, ..., 0.3
k	Kinetic mixing coefficient	$5 \times (10^{-2}, 10^{-1.6}, 10^{-1.2}, ..., 10^{-0.4})$
p_1	Prob. a T cell reacts cytotoxically to a cancer cell	0.3, 04, 0.5, ..., 0.9
p_2	Prob. a T cell does not react cytotoxically to a cancer cell	$1 - p_1$
$\tilde{p}_1$	Prob. a cancer cell dies due to an interaction with a T cell	p_1
n	Average number of T cell division after stimulation	1, 1.5, 2, ..., 4
q_1	Prob. a T cell starts dividing after a cytotoxic response	0.3, 0.4, 0.5, ..., 0.9
q_2	Prob. a T cell does not divide after a cytotoxic response	$1 - q_1$
r_C	Growth rate of cancer	$3 \times (10^{-2}, 10^{-1.9}, 10^{-1.8}, ..., 10^{-1})$
K	Logistic carrying capacity of the cancer population	200, 210, 220, ..., 300

TABLE I

PARAMETER TEST VALUES USED IN SECTION IV-C. WE SCAN OVER ALL POSSIBLE COMBINATIONS OF THESE VALUES.

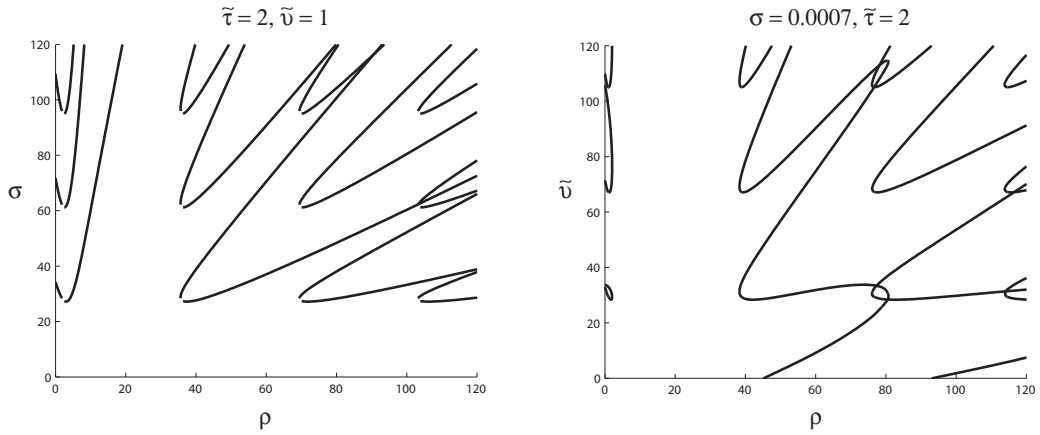

Fig. 3. Crossing curves for σ vs. ρ and υ vs. ρ for given values of (τ, υ) and (σ, τ) respectively.

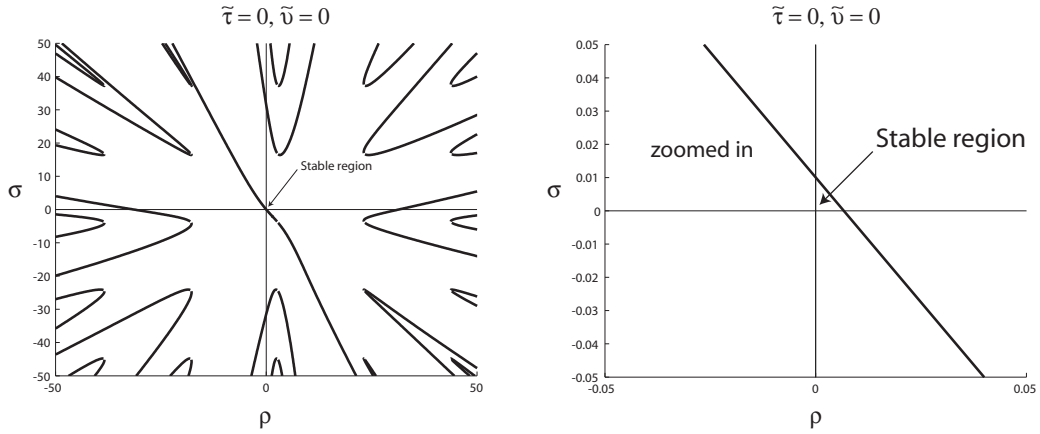

Fig. 4. Crossing curves for σ vs. ρ with $(\tau, \upsilon) = (0, 0)$ for the linearization of (3) around fixed point III, $\left(\frac{c_1 - c_2 b_1/b}{c_3}, \frac{b_1}{b}\right)$.

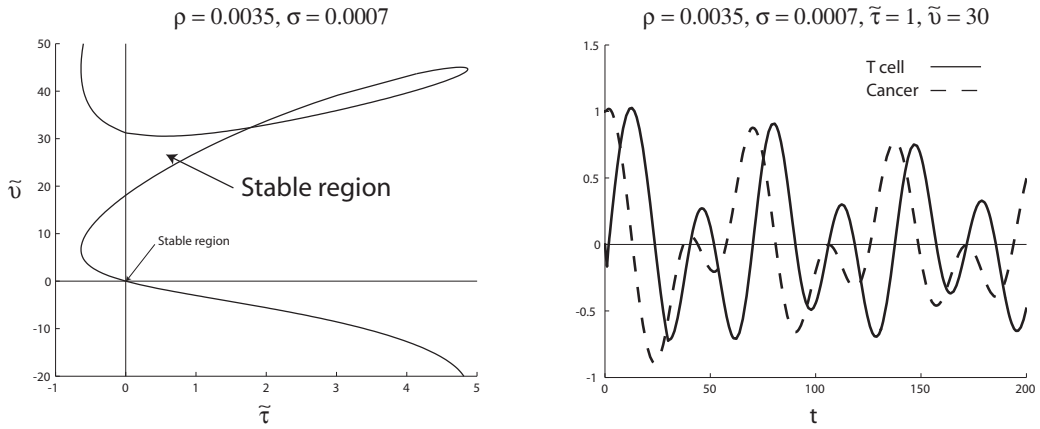

Fig. 5. Left: Crossing curves for υ vs. τ with $(\rho, \sigma) = (0.0035, 0.0007)$. Right: Solution of (4) around fixed point III.

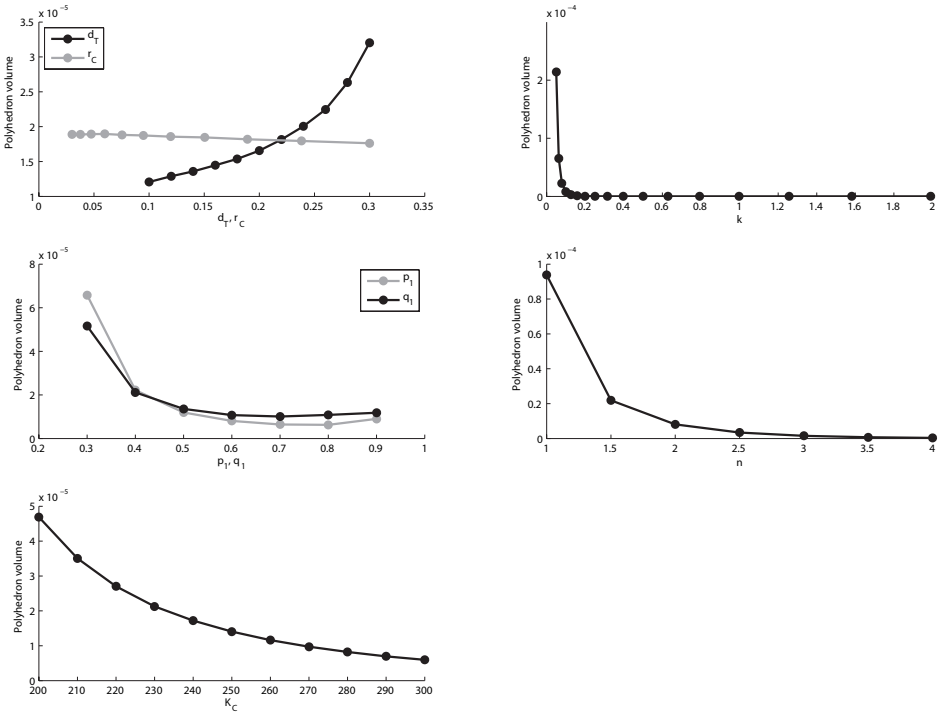

Fig. 6. Average polyhedron volumes vs. individual parameter values

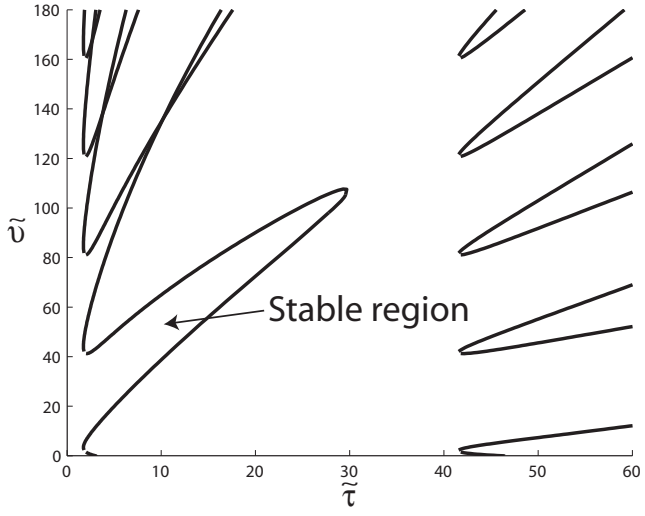

Fig. 7. Crossing curves for $\tilde{v}$ vs. $\tilde{\tau}$ with $k = 0.01$, $d_T = 0.5$, all other parameters according to the estimates in (33), and $(\rho, \sigma) = (0.0035, 0.0007)$.